

## Proposal for threedimensional internal field mapping by cw electrooptic probing

Y. H. Lo, M. C. Wu, Z. H. Zhu, S. Y. Wang, and S. Wang

Citation: [Applied Physics Letters](#) **50**, 1791 (1987); doi: 10.1063/1.97698

View online: <http://dx.doi.org/10.1063/1.97698>

View Table of Contents: <http://scitation.aip.org/content/aip/journal/apl/50/25?ver=pdfcov>

Published by the [AIP Publishing](#)

---

### Articles you may be interested in

[Polarization dependent Bragg diffraction and electro-optic switching of three-dimensional assemblies of nematic liquid crystal droplets](#)

Appl. Phys. Lett. **88**, 121911 (2006); 10.1063/1.2187430

[Tetrahertz near-field electro-optic probe based on a microresonator](#)

Appl. Phys. Lett. **88**, 091118 (2006); 10.1063/1.2176861

[Three-dimensional electric-field mapping system using crystal principal axes electro-optic rotation](#)

Rev. Sci. Instrum. **76**, 055111 (2005); 10.1063/1.1903143

[Electro-optic field mapping system utilizing external gallium arsenide probes](#)

Appl. Phys. Lett. **77**, 486 (2000); 10.1063/1.127019

[New measurement technique: cw electrooptic probing of electric fields](#)

Appl. Phys. Lett. **49**, 432 (1986); 10.1063/1.97636

---



**AIP** | Journal of  
Applied Physics

*Journal of Applied Physics* is pleased to  
announce **André Anders** as its new Editor-in-Chief

# Proposal for three-dimensional internal field mapping by cw electro-optic probing

Y. H. Lo, M. C. Wu, Z. H. Zhu,<sup>a)</sup> S. Y. Wang,<sup>b)</sup> and S. Wang

Department of Electrical Engineering and Computer Sciences, and Electronics Research Laboratory, University of California, Berkeley, California 94720

(Received 16 January 1987; accepted for publication 21 April 1987)

The cw electro-optic probing technique is for the first time proposed to detect the three-dimensional internal field distribution in linear electro-optic material like GaAs. By changing the incident angles and positions of the probing beam, sufficient information of the electric field distribution is included in the phase retardation of the probing beam. If certain conditions on the probing beam are satisfied, a very simple linear relation between phase retardation and each field component can be found and the whole problem becomes not only mathematically solvable but experimentally feasible. Finally, a three-dimensional computer simulation is undertaken to illustrate the relation between field distribution and detected electro-optic signal.

To understand the physics of more and more complicated III-V compound devices and to find out proper physical models to describe or predict the device performance, it is essential to know the internal potential, field, and charge distributions. However, there is no technique presently available to detect such crucial information in either bulk semiconductor or devices. For those compound materials having linear electro-optic properties such as GaAs, the phase retardation of light is affected by the electric field inside the material, and thus intrinsically contains the information of electric field in the area swept by the probing light. This attractive property has been widely applied to detect the logic state and transient response of a very fast GaAs circuit,<sup>1-5</sup> or in cw operation, to detect the surface potential variation and the boundary of a *p-n* junction.<sup>6,7</sup> However, none of the work has ever explored the possibility of the great importance of extracting three-dimensional internal field distribution from the electro-optic signals. In this letter, we propose for the first time a nondestructive, high-resolution three-dimensional field measurement method by means of the cw electro-optic probing (CWEOP).

Because GaAs is the most extensively used electronic and optic material having linear electro-optic effect, we will consider it as an example in this paper. The index ellipsoid of GaAs under the electric field is described in Eq. (1).

$$(x^2 + y^2 + z^2)/n_0^2 + 2\gamma_{41}(E_x yz + E_y zx + E_z xy) = 1, \quad (1)$$

where  $\gamma_{41}$  is the only nontrivial electro-optic coefficient for the cubic crystal GaAs. If the wave vector  $\mathbf{k}$  of the probing laser beam has directional cosines  $\alpha, \beta, \gamma$  with respect to the three crystal axes, the plane normal to  $\mathbf{k}$  and passing through the origin is described as Eq. (2).

$$\alpha x + \beta y + \gamma z = 0. \quad (2)$$

Geometrically, those points satisfying both Eqs. (1) and (2) form an ellipse  $C$  normal to  $\mathbf{k}$  as shown in Fig. 1. The direc-

tions of the major and minor axes of the ellipses represent two eigenvectors of the polarization states of the light, and their magnitudes are equal to the refraction indices of the slow and fast optical axes. In spite of the clarity in geometry, the algebra to find those two axes is very involved. However, if the  $\mathbf{k}$  is in the *y-z* plane and the angle with the *z* axis is less than  $45^\circ$ , the problem can be greatly simplified. These conditions are satisfied for all the following derivations and proposed measurements. The simplest mathematical approach is to first project the ellipse  $C$  normal to  $\mathbf{k}$  into an ellipse  $C'$  in the *x-y* plane as shown in Fig. 1.

After obtaining the directions and magnitudes of the axes of  $C'$  in the way of planar analytic geometry, we can easily find the axes of ellipse  $C$  by Eq. (2) since each point in  $C'$  possesses the same *x* and *y* coordinates as the corresponding point in  $C$ . The results are summarized in the following set of equations:

$$\cot(2\theta) \equiv \xi = (2a + c)/d, \quad (3)$$

where

$$a = (\alpha^2)/(\gamma^2) - 2n_0^2(\alpha/\gamma)\gamma_{41}E_y, \quad (4a)$$

$$c = 2n_0^2\gamma_{41}(\alpha E_y + \beta E_x)/\gamma - (\alpha^2 + \beta^2)/\gamma^2, \quad (4b)$$

$$d = 2[(\alpha\beta)/\gamma^2 + n_0^2\gamma_{41}(\gamma E_z - \alpha E_x - \beta E_y)/\gamma]. \quad (4c)$$

The angle  $\theta$  in Eq. (3) is the angle between the *x* axis and the

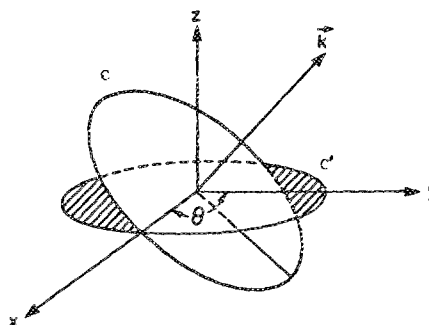


FIG. 1. Configuration of the index ellipse  $C$  normal to the wave vector  $\mathbf{k}$  and its projection  $C'$  in the *x-y* plane.  $\theta$  is the acute angle between the axis (major or minor) of  $C'$  and the *x* axis.

<sup>a)</sup> Permanent address: Department of Radio and Electronic Engineering, Zhejiang University, Hangzhou, China.

<sup>b)</sup> Permanent address: Hewlett-Packard Laboratories, Palo Alto, CA.

axis (major or minor) of ellipse  $C'$  such that  $0 < \theta \ll (\pi/2)$ . The directional cosines  $\alpha, \beta, \gamma$  are those of  $\mathbf{k}$ . The two extrema of the ellipse normal to  $\mathbf{k}$  have the coordinates described as follows:

$$x_{\pm} = n_0 \cos \theta \sqrt{(1+c') \pm d'}, \quad (5a)$$

$$y_{\pm} = n_0 \sin \theta \sqrt{(1+c') \pm d'}, \quad (5b)$$

$$z_{\pm} = -(\alpha x_{\pm} + \beta y_{\pm})/\gamma, \quad (5c)$$

and

$$n_{\pm} = \sqrt{x_{\pm}^2 + y_{\pm}^2 + z_{\pm}^2} \\ = n_0 \sqrt{(1+c') \pm d'} \left( 1 + \frac{(\alpha \cos \theta - \beta \sin \theta)^2}{\gamma^2} \right), \quad (6)$$

where  $c' = c/2$  and  $d' = d/[2 \sin(2\theta)]$ .

After finding the field dependence of the eigenstates for arbitrary incident light, we look for the relation between the detected variation and spatial distribution of electric field by the prescribed electro-optic effect. For simplicity but without loss of generality, let us assume the probing light initially linearly polarized along the  $x$  axis, and then its polarization state can be represented by the Jones vector as

$$J = \begin{bmatrix} 1 \\ 0 \end{bmatrix}. \quad (7)$$

To find the field distribution from a finite number of probing beams, we need to set up the mesh points in the tested area. For each small unit of those meshes, the transformation of the polarization state from input beam to output beam is described as follows<sup>8</sup>:

$$\begin{bmatrix} J_{xi} \\ J_{yi} \end{bmatrix} = e^{-i\Delta_i} R_i^{-1} \begin{bmatrix} e^{-i\Gamma_i/2} & 0 \\ 0 & e^{i\Gamma_i/2} \end{bmatrix} \\ \times R_i \begin{bmatrix} J_{xi-1} \\ J_{yi-1} \end{bmatrix} = W_i \begin{bmatrix} J_{xi-1} \\ J_{yi-1} \end{bmatrix}, \quad (8)$$

$$R_i = \begin{bmatrix} \cos \Phi_i & \sin \Phi_i \\ -\sin \Phi_i & \cos \Phi_i \end{bmatrix}, \quad (9)$$

$$\Gamma_i = (\omega l_i/c)(n_{si} - n_{fi}), \quad (10)$$

$$\Delta_i = (\omega l_i/2c)(n_{si} + n_{fi}), \quad (11)$$

where  $R_i$  is the matrix rotating the initial polarization state, along  $x$  axis in this case, to the slow axis of the index ellipse. The quantity  $\Gamma_i$  is the phase retardation, and  $n_{si}$  and  $n_{fi}$  are slow and fast refraction indices of the  $i$ th mesh, and  $l_i$  is the length of the optical path in mesh  $i$ . Because the  $\exp(-i\Delta_i)$  term in Eq. (8) does not have any physical significance but a phase shift, we will omit it in the following derivations.

If the  $y$  component of the polarization state is detected from the emerging beam, the final  $J_{yk}$  is obtained from a series of multiplication of the transformation matrices  $W_i$  in Eq. (8) along the light path.<sup>8</sup>

$$J_{yk} = \frac{-i}{2} \sum_i \Gamma_i \sin(2\Phi_i), \quad (12)$$

where the summation is over all the mesh points passed by the probing beam with wave vector  $\mathbf{k}$ . In Eq. (12), we have approximated  $\exp(-i\Gamma_i) \approx 1 - i\Gamma_i$  since the phase retardation in each mesh is always much smaller than one radian.

In general, both  $\Gamma_i$  and  $\Phi_i$  in Eq. (12) are functions of  $E_{xi}$ ,  $E_{yi}$ , and  $E_{zi}$  resulting in a number of cross terms in Eq. (12). To simplify the analysis, we must choose the incident beam to be either in  $y$ - $z$  plane or in  $x$ - $z$  plane (i.e.,  $\alpha = 0$  or  $\beta = 0$ ). Assuming  $\mathbf{k}$  in  $y$ - $z$  plane (i.e.,  $\alpha = 0$ ) as an example, we simply set  $\Phi_i$  in Eqs. (9) and (12) equal to  $\theta_i$  in Eq. (3) if  $d$  in Eq. (4c)  $> 0$  or equal to  $\theta_i + \pi/2$  if  $d < 0$ . The  $\pi/2$  difference between  $\Phi_i$  and  $\theta_i$  as  $d < 0$  is due to the previous definition that the angle  $\Phi_i$  is between  $x$  axis and the slow axis but  $\theta_i$  is confined in  $(0, \pi/2)$  to ensure  $\sin(2\theta_i)$  in Eq. (6) larger than zero. By combining Eqs. (3), (4), (6), (10), and (12) and the above relation between  $\theta_i$  and  $\Phi_i$  with the condition  $\alpha = 0$ ,  $J_{yk}$  can be explicitly represented in terms of the field components as follows:

$$J_{yk} = \frac{K}{|\gamma|} \sum_i \left( E_{zi} - \frac{\beta}{\gamma} E_{yi} \right) \left[ 1 + \left( \frac{\beta}{\gamma} \right)^2 \sin^2 \theta_i \right]^{1/2}, \quad (13)$$

$$K = -i(\omega l_0 n_0^3 \gamma_{41})/(2c). \quad (14)$$

The field-dependent nonlinear term in the square root of Eq. (13) is negligible as long as the incident beam has a small angle with the  $z$  axis, in other words,  $\beta^2/\gamma^2 \ll 1$ . Therefore, Eq. (13) can be approximated as

$$J_{yk} \approx \frac{K}{|\gamma|} \sum_i \left( E_{zi} - \frac{\beta}{\gamma} E_{yi} \right). \quad (15)$$

Equation (15) is the equation setting up the linear relation between the field components and the detected probing beam from different angles and positions. The  $E_{xi}$  in Eq. (15) is missing because of the condition  $\alpha = 0$ . To find  $E_{xi}$ , we can replace  $\beta E_{yi}$  with  $\alpha E_{xi}$  in Eq. (15) assuming that the light is in  $x$ - $z$  plane. The signal from a photodetector is proportional to the magnitude of  $J_{yk}$  based on the same principle as the amplitude modulation of electro-optic material.<sup>9</sup> Therefore, the three-dimensional electric field distribution measurement becomes not only theoretically possible but practically feasible by means of the recently developed cw electro-optic probing technique.<sup>6,7</sup> From the measured field distribution, the real values of potential profile, field intensity, and charge density can be substantially obtained since the applied voltage supplies the necessary boundary conditions.

Figure 2(c) shows the computer simulation results of the electro-optic signals from Eq. (15) under some given  $E_y$ ,  $E_z$  distributions shown in Figs. 2(a) and 2(b). The detected area in Fig. 2 is  $100 \times 100 \mu\text{m}^2$  in the  $y$ - $z$  plane and the incident probing beam scans from  $-18^\circ$  to  $18^\circ$  with  $1^\circ$  difference between adjacent beams. Not only does the beam incident angle vary, the probing beam also moves along the  $y$  axis with  $0.18 \mu\text{m}$  per step to supply enough linearly independent equations to solve the field components at each mesh point. A larger mesh size can be used in those regions of slow-varying field to reduce the number of probing beams and save computer memories without sacrificing the accuracy. Finally, a simple experiment is done to justify our proposed method in practice. As shown in Fig. 3, the electro-optic signals measured under normal incidence and  $1.4^\circ$  tilted incidence are clearly distinguishable. Those features occurring in the tilted incidence curve are partly due to the different optical path from the normal incident one and partly due to

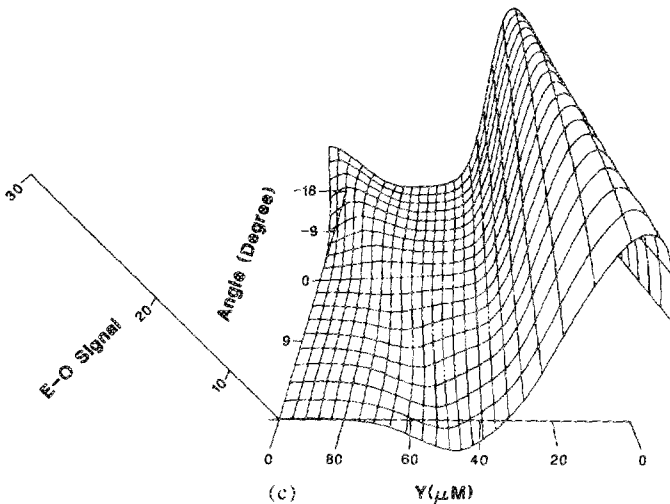
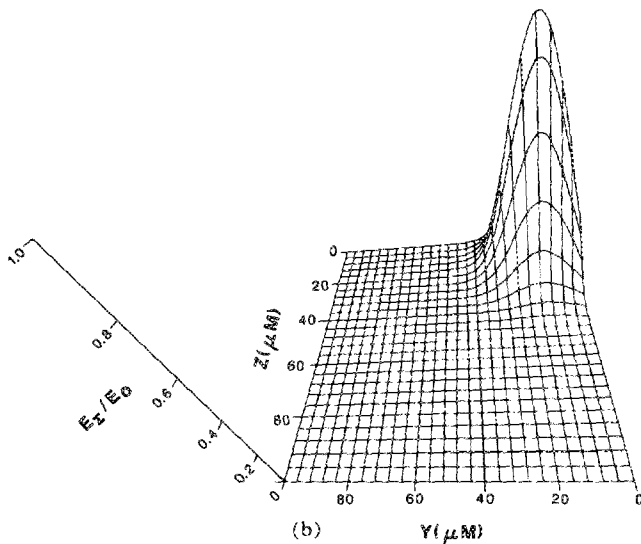
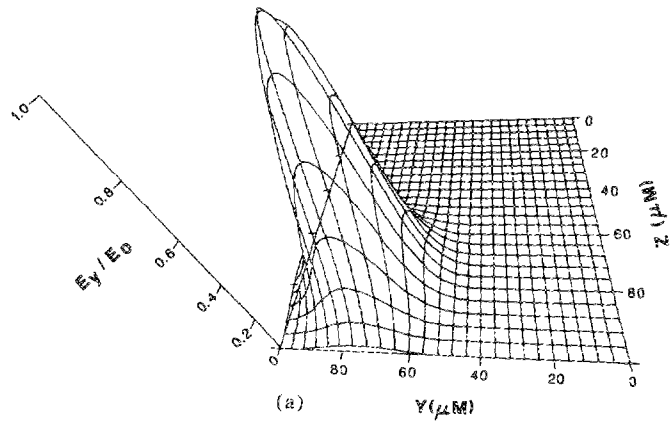


FIG. 2. Computer simulation of the electro-optic signal under the given field profile in  $y$ - $z$  plane.  $E_y$  and  $E_z$  profiles are shown in (a) and (b) but  $E_x$  is not shown here because it does not affect the electro-optic signal if the light has the wave vector in the  $y$ - $z$  plane; (c) shows the signal variation as both the incident angle and the incident position along the  $y$  axis change.

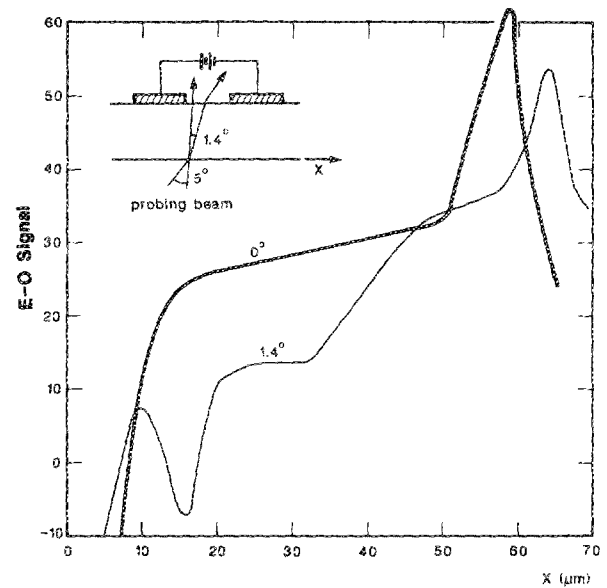


FIG. 3. Measured electro-optic signal across two electrodes on GaAs substrate. The dark curve is measured under normal incidence and the light one is measured under incidence at an angle. Lock-in technique is used in this experiment.

the influence of lateral field. The more complete experiment and the detailed analysis of the experimental data will be published elsewhere.

In conclusion, we propose a very new method to nondestructively detect the three-dimensional field distribution in linearly electro-optic materials such as GaAs, and mathematically formulate it. If an appropriate incident angle is chosen, the electro-optic signal is a linear combination of the field components in the light path. This property facilitates the data analysis and makes the experiment more feasible. To obtain more accurate results, the finite beam spot size, multiple reflection inside the material, reflection at the interface, as well as the light shape function all need to be taken into account.

The authors are grateful to J. Y. Fang for his generous help in computer graphics. This work is supported in part by Bell Communications Research and by Joint Services Electronics Program AFOSR F49620-84-C-0057.

- <sup>1</sup>B. H. Kolner and D. M. Bloom, *IEEE J. Quantum Electron.* **QE-22**, 69 (1986).
- <sup>2</sup>J. L. Freeman, S. K. Diamond, H. Fong, and D. M. Bloom, *Appl. Phys. Lett.* **47**, 1083 (1985).
- <sup>3</sup>K. Stenersen and R. K. Jain, *IEEE Electron Device Lett.* **EDL-5**, 422 (1984).
- <sup>4</sup>A. J. Taylor, J. M. Wiesenfeld, R. S. Tucker, G. Eisenstein, J. R. Talman, and U. Koren, *Conference on Lasers and Electro-Optics Technical Digest* 312 (1986).
- <sup>5</sup>R. K. Jian, X-C. Zhang, M. G. Ressi, and T. J. Pier, *Conference on Lasers and Electro-Optics Technical Digest* 312 (1986).
- <sup>6</sup>Z. H. Zhu, J. -P. Weber, S. Y. Wang, and S. Wang, *Appl. Phys. Lett.* **49**, 432 (1986).
- <sup>7</sup>Y. H. Lo, Z. H. Zhu, C. L. Pan, S. Y. Wang, and S. Wang, *Appl. Phys. Lett.* **50**, 1125 (1987).
- <sup>8</sup>A. Yariv and P. Yeh, *Optical Waves in Crystals* (Wiley, New York, 1984), pp. 121-125.
- <sup>9</sup>A. Yariv, *Quantum Electronics* (Wiley, New York, 1975), pp. 339-341.